Direct acoustic vector field mapping: new scanning tools for measuring 3D sound intensity in 3D space

Daniel Fernandez Comesaña, Steven Steltenpool, Marcin Korbasiewicz and Emiel Tijs
Microflown Technologies, Tivolilaan 205, Arnhem, the Netherlands
email: fernandez@microflown.com.

Summary
One of the main challenges arising from noise and vibration problems is how to identify the areas of a device, machine or structure that produce significant acoustic excitation. Measurement methods relying on sound intensity are widely used for the localization and quantification of noise sources although they are often limited by the measurement environment. In contrast, the use of a microphone in combination with three orthogonal particle velocity sensors enables the direct acquisition of 3D dimensional sound intensity without the traditional frequency constrains of pressure-based solutions. Furthermore, stationary sound fields can be characterized efficiently by means of manual scanning techniques. In this paper, a expanded scanning method is used in combination with a 3D tracking system based on a stereo camera. Acoustic variations throughout space can be then determined by combining the signals acquired with the tracking information of the probe. An overview of the measurement methodology is given along with the evaluation of several practical examples.

PACS no. 43.58.-e, 47.80.-v

1. Introduction

The transformation of physical phenomena into something visual has provided fundamental insight to the develop of many fields of science throughout history. Particularly, in acoustics, sound visual representations have been thought of as a key to aid in understanding [1, 2]. The visualization of vectorial fields has changed the approach to examining many acoustic problems, greatly simplifying research methods [3]. The spatial distribution of sound intensity can be used to depict various acoustic phenomena. In sound engineering, it may be an acoustic wave power density distribution, wave dissipations or the evaluation of wave motion within a medium. For experimental acoustics, the directional characteristics of industrial sources, near-field effects and variables associated with reflection, scattering and diffractions due to obstacles could prove interesting.

Sound visualization tests usually involve a large number of intensity measurements. The early methods used point-by-point measurements to acquire sound intensity at several positions, resulting in a rather time-consuming process [3]. In [4] a fast procedure was introduced, using an optical camera to track the position of a probe that is manually scanned through a plane. However, the position in the plane and the orientation of the probe are hard to control accurately. In [5], a method was presented to capture the 3D position and orientation of the sensor, allowing free movement of the intensity probe.

For many years sound intensity has been measured almost exclusively using pair(s) of closely spaced microphones, i.e. with *p-p* probes. Nowadays, intensity can also be measured with *p-u* probes consisting of a microphone and one or multiple particle velocity sensors. Unlike *p-p* probes, *p-u* probes cover the full audible frequency range, have reduced dimensions, can easily be extended to full 3D probes, and can be used in environments with high levels of background noise or reflections [6, 7]. These characteristics make *p-u* probes very attractive for many practical applications.

The novel scan-based sound visualization technique introduced in this paper is an adaptation of the 2D technique “Scan & Paint" [4, 8]. In our case, the 3D intensity probe is manually moved whilst a stereo camera is used to extract the instantaneous position of the sensor in the three dimensional space. The recorded signals are split into multiple segments and assigned to a set of positions using a spatial discretization algorithm. A vector representation of the acoustic variations across the sound field can then be computed using combinations of the sound pressure and the three orthogonal acoustic particle velocities. Results are presented over a 3D sketch of the tested object, obtaining a visual representation of the sound distribution around the object.

Firstly, a brief overview of the theoretical considerations that have to be taken into account for computing sound intensity using a three dimensional *p-u* probe is given. Next, the measurement methodology is introduced along with the spatial discretization algorithm implemented. Finally, two practical examples are investigated: a loudspeaker cabinet and a window wiper actuator.

2. Three dimensional sound intensity using a *p-u* probe

Sound intensity is "a measure of the flow of acoustic energy in a sound field" [9]. It provides not only a quantification of the acoustic emission but also the direction of sound propagation. The instantaneous sound intensity is defined as the product of sound pressure and acoustic particle velocity as such

$$\mathbf{I}(t) = p(t)\,\mathbf{u}(t) \tag{1}$$

Sound pressure and acoustic particle velocity have a phase difference which mainly depends upon the characteristic of the sound source and the measurement distance [10]. This implies that the instantaneous products of the sound pressure and each orthogonal particle velocity component yields a complex vector: the complex acoustic intensity **C**. The imaginary part of this quantity is known as the reactive intensity **J**, which represents the non-propagating acoustic energy. It is, however, more common to study stationary sound fields in terms of the active, or propagating, part of the complex intensity averaged over time [11], i.e.

$$\mathbf{I} = \{I_x, I_y, I_z\} = < p\,\mathbf{u} >_t = \frac{1}{2}\mathrm{Re}\{p\,\mathbf{u}\} \tag{2}$$

where $< \, . \, >_t$ indicates time averaging. Figure 1 shows a schematic representation of the one dimensional complex acoustic intensity and the modulus of the three-dimensional active intensity vector where $\theta_p - \theta_{u_n}$ represents the phase difference between pressure and particle velocity.

Sound pressure and the acoustic particle velocity vector can be directly acquired using a *p-u* probe comprising a microphone and three orthogonally placed particle velocity sensors (also known as a Microflowns), or estimated via indirect methods, using a *p-p* probe to approximate acoustic particle velocity from the gradient between two microphones. Multiple research articles have been published exploring the fundamental differences between these two sound intensity measurement principles [6, 12, 13]. Pressure-based measurement methods cannot be utilized when

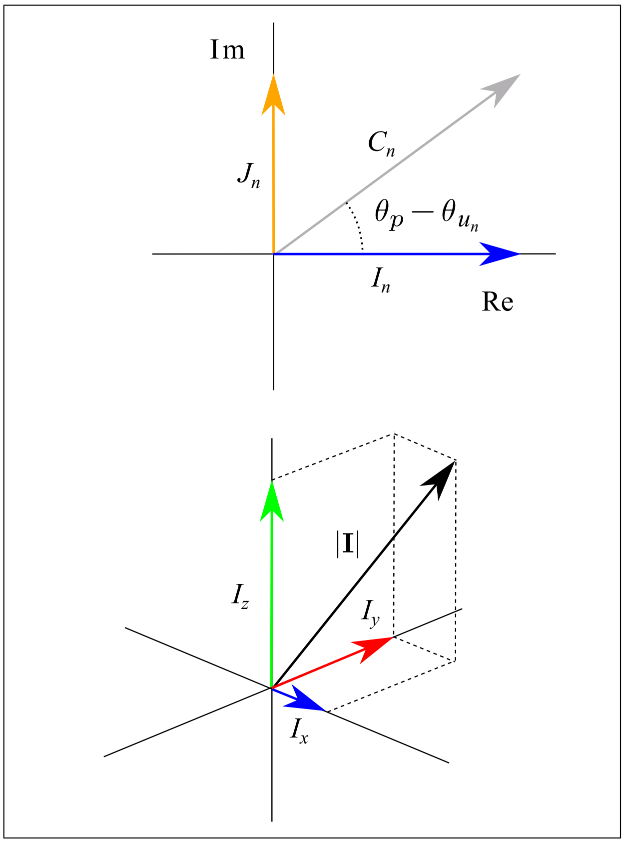

Figure 1. Schematic representation of the one dimensional complex acoustic intensity (up) and the three dimensional active intensity (down).

the pressure-intensity index (the ratio of sound pressure squared to active intensity) is high, which in practice limits the use of *p-p* intensity probes in environments with high levels of background noise or reflections (a detailed analysis of this phenomena is described in [14]). In contrast, direct intensity measurements using a combination of pressure and particle velocity transducers, the so called *p-u* intensity probes, are unaffected by this index, enabling the estimation of propagating acoustic energy despite unfavorable conditions [6, 7]. On the other hand, the error of the intensity calculations using *p-u* probes mainly depends upon the reactivity of the sound field and the calibration of the probe [6]

$$\hat{I}_n \cong I_n\left(1 + \varphi_{ue}\frac{J_n}{I_n}\right) = I_n(1 + b[\hat{I}_n]) \tag{3}$$

where φ_{ue} is a small phase error introduced during the calibration procedure and J_n is the reactive intensity, defined as

$$J_n = \frac{1}{2}\mathrm{Im}\{p u_n^*\} \tag{4}$$

If the reactivity is high, for example in the near field of a source, a small phase mismatch in the transducer's calibration may lead to considerable error in the intensity estimate. In [14] it is stated that in practical situations the reactive intensity should not exceed the active intensity by more than 5 dB, which corresponds to a ±72 degree phase difference between sound pressure and particle velocity. Although active intensity may be biased in a highly reactive field, the phase difference between pressure and particle velocity can still be measured accurately. Therefore, it is still possible to discard measurement positions which are exposed to high reactivity.

3. Sound intensity acquisition in 3D

The sound visualization method hereby introduced is an extension of the technique "Scan & Paint" [4, 8] for a three dimensional domain. This section gives an overview of the two main novel aspects that enable this upgrade: the 3D positioning system and the cuboid grid discretization method.

3.1. Positioning system

It is key to obtain detailed information about both position and orientation of the probe over time for computing the spatial distribution of sound intensity. A stereo camera is used as a tracking system, which measures six degrees of freedom, i.e. the position in three directions (x, y, z) and the three angular coordinates (α, β, γ). Each camera is equipped with an infrared (IR) pass filter in front of the lens and a ring of IR LEDs around the lens to periodically illuminate the measurement space with IR light. An uneven spherical structure with embedded retro-reflective markers is attached to the probe handle in order to track translation and rotation movements of the probe. The IR light reflections are detected by the stereo camera, and the tracking system translates them to exact 3D coordinates along with the sensor orientation. Figure 2 shows a picture of the tracking system together with the intensity probe. In contrast to inertial navigation systems, optical tracking is unaffected by strong electromagnetic fields and it does not have drift error over time. The spatial resolution of the system depends upon the camera view angle, the measurement distance and the amount of reference markers as well as their size. As reported in [5], a tracking error lower than 0.5 mm in position and 1 degree in orientation can be achieved using a grid of 7 mm diameter markers in a range of 2.5 m distance from the tracking system. The tracking can be done real time and with a maximum sample rate of 120 Hz. An example of the tracking extracted from a measurement of a loudspeaker is shown in Figure 3.

3.2. Spatial discretization

One of the key steps of the sound visualization method proposed is the fragmentation of the continuously acquired data. It is essential to define a method that

Figure 2. Stereo camera system for tracking the movement of the spherical structure attached to a 3D intensity probe.

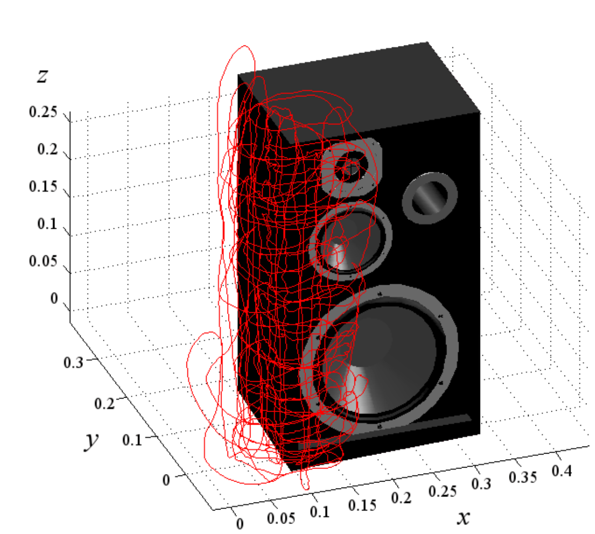

Figure 3. Example of the tracking path followed during the measurement.

guarantees the robustness and accuracy of the data splitting process.The regular discretization of a continuous spatial domain is often used by many computational acoustic techniques, such as FEM [15] or FDTD [16]. It provides a decomposition of a continuous domain into a finite set of equal sized elements. As a result, the resolution and accuracy are preserved across the space, achieving homogeneous estimations across the entire three dimensional space. Once the spatial domain of interest has been discretized, a link can be then established between measurement data acquired with a moving transducer and the defined grid. The continuous path followed by the sensor is fragmented into several segments using the grid structure hence dividing the original signal and assigning each segment a position in the measurement volume. One grid cell can have multiple associated sections of the original signal if the probe crosses the same volume several times. Averaging is therefore required if multiple time signals are associated to a single cell. A detailed description of the mathematical derivation of an analogous method for 2 dimensional space can be found in [8].

4. Experimental evaluation

The direct mapping of a vector quantity, particularly the visualisation of sound intensity, contributes to a more comprehensive interpretation of acoustic radiation mechanisms. Experimental evidence can be used to understand how the acoustic field is excited, potentially helping to improve the acoustic characteristics of the assessed device. Two experimental cases are presented in this section: a loudspeaker and an small actuator. The sound fields are illustrated using a 3D model of the sound source overlaid with the measured sound intensity vector field.

4.1. Loudspeaker

In this first practical example the sound field produced by a complex structure, a 3-way loudspeaker, is evaluated in an office environment. The aim of this test was to investigate the radiation pattern and near field interactions between drivers as well as to visualize the impact of the edges of the cabinet on the sound radiation. Two scanning measurements of approximately 8 minutes were undertaken in the vicinity of the loudspeaker. A spatial discretization grid with cubic cells of 5 mm size was applied. As a result, Figure 4 illustrates the woofer and the mid-high driver iteration evaluated in the frequency band from 1780 Hz and 1875 Hz. As shown, a constructive interference is produced between the two main drivers active on this range. Furthermore, an interesting phenomenon can be seen at the sides of the cabinet. The local minima and maxima along the cabinet side are most likely to appear due to an interference effect between the two drivers and a reflection on the floor of the room.

4.2. Window wiper actuator

This section is focused on the investigation of actuators for window wipers used in the automotive industry. The acoustic sound field generated by a defective window wiper actuator is studied and compared to a fully functional unit. The Scan & Paint 3D system is used to visualize particle velocity distribution as well as the sound intensity vectors in order to detect and rank the noise source of the actuators and localize the defect. In this case, a frequency range between 4100 and 4600 Hz was identified as the main range of interest which allows for the differentiation between the noisy and the regular actuator. Figure 5 shows the averaged sound intensity spectrum recorded over both window wiper actuators. One scanning measurement of approximately 4 minutes was carried out for each device. A set of sound intensity vectors spaced by 10 mm was obtained after the application of the spatial discretization filter. As shown, the noise produced by the defective actuator is approximately 10 dB louder than the noise of the normal unit. The sound intensity field clearly shows the origin of the noise radiation.

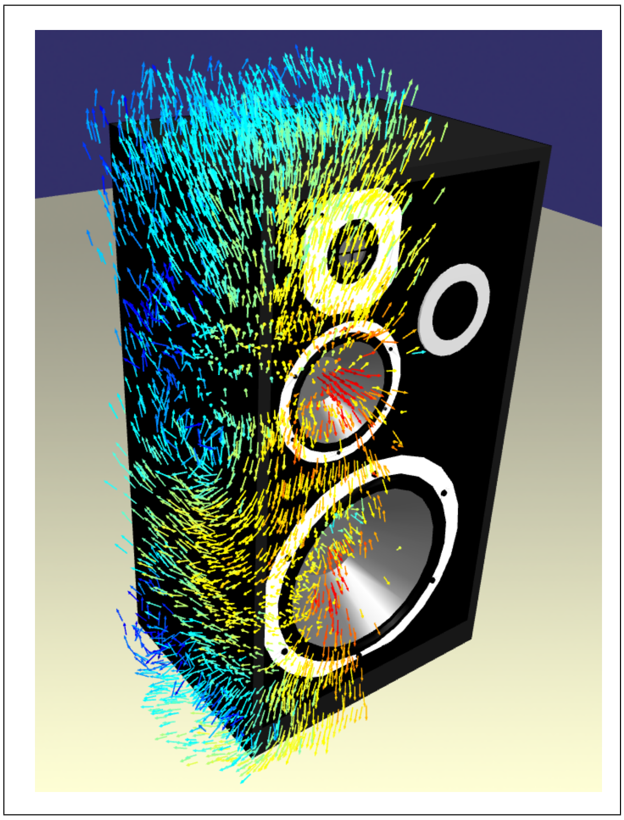

Figure 4. Sound intensity distribution along the edge of the cabinet between 1780 Hz and 1875 Hz.

5. Conclusions

A novel scan-based measurement technique to characterise the sound energy distributions in a fast and efficient way is presented. The use of a 3D p-u intensity probe along with a 3D tracking system enables to acquire high resolution sound intensity maps without specific restriction on the frequency range or conditions of the testing environment. Furthermore, this research has aided the development of a commercially available 3D sound intensity measurement system.

Results of two different tests have been presented. The sound maps obtained provide key insight on how sound interacts in the vicinity of the evaluated objects. The visualization of sound can be helpful not only for characterizing complex noise sources but also for designing effective noise reduction strategies.

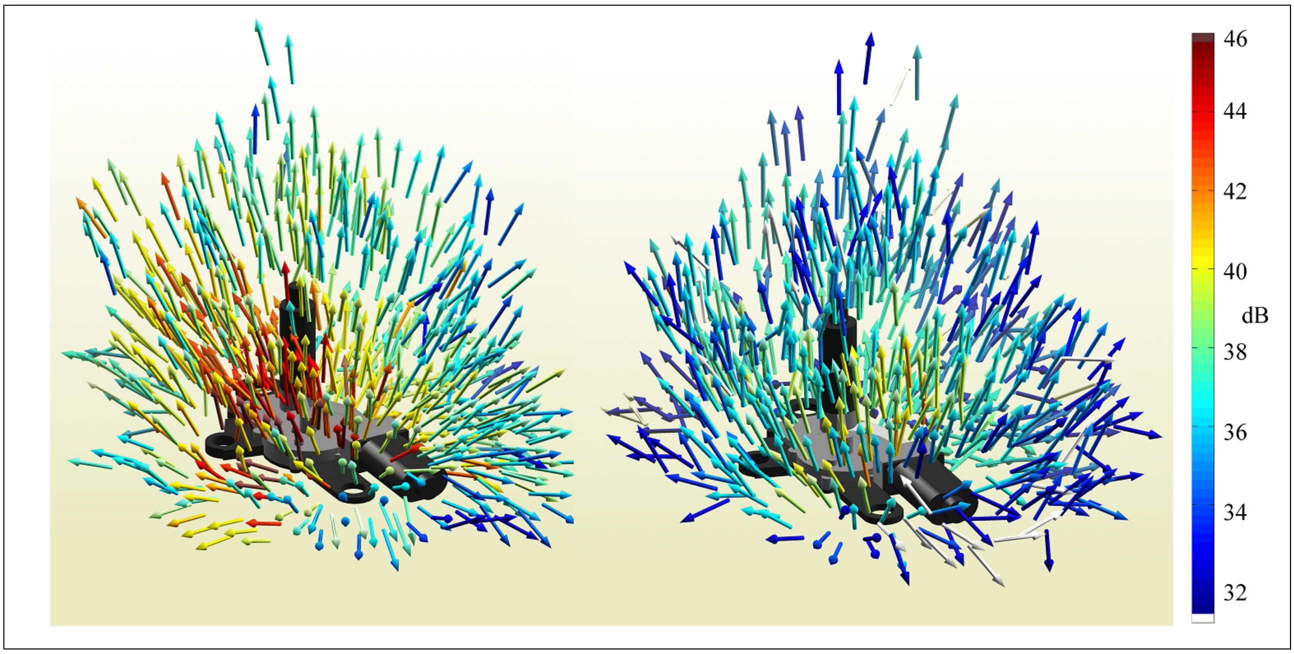

Figure 5. Sound intensity distribution in the frequency range between 4100 and 4600 Hz, of a defective actuator (left) and a functional actuator (right).

References

[1] W.E. Kock. *Seeing sound*. Wiley-Interscience, 1971.

[2] R.T. Beyer. *Sounds of Our Times: Two Hundred Years of Acoustics*. Springer Verlag GMBH, 1999.

[3] S. Weyna. Acoustic flow visualization based on the particle velocity measurements. In *Forum Acousticum*, 2005.

[4] Daniel Fernandez Comesaña, Emiel Tijs, Peter Cats, and Douglas Cook. Visualization of acoustic intensity vector fields using scanning measurement techniques. In *Internoise 2013*, September 2013.

[5] E.H.G. Tijs, W.J.M. Koomen, and A.J. Brinkman. Rapid high resolution 3d intensity measurements with a stereo camera system. In *DAGA*, 2014.

[6] Finn Jacobsen and Hans-Elias de Bree. A comparison of two different sound intensity measurement principles. *J. Acoust. Soc. Am.*, 118(3): 1510–1517, 2005.

[7] W. F. Druyvesteyn and H. E. de Bree. A new sound intensity probe comparison with the pair of pressure microphones intensity probe. *J. Audio Eng. Soc*, 48(1/2):49–56, 2000.

[8] D. Fernandez Comesaña, S. Steltenpool, G. Carrillo Pousa, H-E. de Bree, and K. Holland. Scan and paint: theory and practice of a sound field visualization method. *ISRN Mechanical Engineering*, 2013(241958):1–11, 2013.

[9] F. Jacobsen and P.M. Juhl. *Fundamentals of General Linear Acoustics*. Wiley, 2013.

[10] L. E. Kinsler, A. R. Frey, A. B. Coppens, and J. V. Sanders. *Fundamentals of acoustics*. Wiley, 2000.

[11] F. Fahy. *Sound Intensity*. E & FN Spon, 1995.

[12] E. Tijs, Nejade A., and H-E. de Bree. verification of p-u intensity calculation. In *Novem*, 2009.

[13] W. F. Druyvesteyn and H. E. de Bree. A new sound intensity probe: Comparison to the Bruel & Kjaer p-p probe. In *Audio Eng. Soc. Conv. 104*, 1998.

[14] Finn Jacobsen and Hans-Elias De Bree. Measurement of sound intensity: P-U probes versus P-P probes. In *NOVEM*, 2005.

[15] M.J. Crocker. *Handbook of Noise and Vibration Control*. Wiley InterScience. Wiley, 2007.

[16] J. B. Schneider. Understanding the Finite-Difference Time-Domain method, 2010. URL `www.eecs.wsu.edu/ schneidj/ufdtd`.